

**RESEARCH ARTICLE**

10.1029/2018JF004617

**Key Points:**

- Morphological changes induced by marsh lateral erosion affect tidal dynamics in estuarine systems
- Positive feedback between marsh loss and reduction in sediment trapping capacity of estuarine systems
- Effects of marsh loss on sediment budget destinations

**Supporting Information:**

- Supporting Information S1

**Correspondence to:**

C. Donatelli,  
carmine@liverpool.ac.uk

**Citation:**

Donatelli, C., Ganju, N. K., Zhang, X., Fagherazzi, S., & Leonardi, N. (2018). Salt marsh loss affects tides and the sediment budget in shallow bays. *Journal of Geophysical Research: Earth Surface*, 123, 2647–2662. <https://doi.org/10.1029/2018JF004617>





Received 10 MAY 2018

Accepted 25 SEP 2018

Accepted article online 29 SEP 2018

Published online 27 OCT 2018

**Salt Marsh Loss Affects Tides and the Sediment Budget in Shallow Bays**

**Carmine Donatelli<sup>1</sup> , Neil Kamal Ganju<sup>2</sup>, Xiaohe Zhang<sup>3</sup> , Sergio Fagherazzi<sup>3</sup> , and Nicoletta Leonardi<sup>1</sup> **

<sup>1</sup>Department of Geography and Planning, School of Environmental Sciences, Faculty of Science and Engineering, University of Liverpool, Liverpool, UK, <sup>2</sup>Woods Hole Coastal and Marine Science Center, U.S. Geological Survey, Woods Hole, MA, USA, <sup>3</sup>Department of Earth Sciences, Boston University, Boston, MA, USA

**Abstract** The current paradigm is that salt marshes and their important ecosystem services are threatened by global climate change; indeed, large marsh losses have been documented worldwide. Morphological changes associated with salt marsh erosion are expected to influence the hydrodynamics and sediment dynamics of coastal systems. Here the influence of salt marsh erosion on the tidal hydrodynamics and sediment storage capability of shallow bays is investigated. Hydrodynamics, sediment transport, and vegetation dynamics are simulated using the numerical framework Coupled Ocean-Atmosphere-Wave-Sediment Transport in the Barnegat Bay-Little Egg Harbor system, USA. We show that salt marsh erosion influences the propagation of tides into back-barrier basins, reducing the periodic inundation and sediment delivery to marsh platforms. As salt marshes erode, the sediment trapping potential of marsh platforms decreases exponentially. In this test case, up to 50% of the sediment mass trapped by vegetation is lost once a quarter of the marsh area is eroded. Similarly, without salt marshes the sediment budget of the entire bay significantly declines. Therefore, a positive feedback might be triggered such that as the salt marsh retreats the sediment storage capacity of the system declines, which could in turn further exacerbate marsh degradation.

**1. Introduction**

Salt marshes are coastal ecosystems generally located in low energy environments, regularly flooded by tides and storm surges, and relying on vegetation for stabilization in response to wave attack and sea level rise (e.g., Allen & Pye, 1992; Boorman, 1995; Fagherazzi et al., 2012). Salt marshes provide several important ecosystem services; for instance, they filter pollutants, act as buffers against coastal storms, serve as nurseries for commercial fisheries, and store significant amounts of carbon and sediment on a geological time scale (e.g., Costanza et al., 1997). In recent years salt marshes have been the focus of many restoration plans built on the concept of *nature-based solutions* for flood defenses (e.g., Temmerman et al., 2013), which aim to use vegetated surfaces to reduce the impact of storms on coastlines. The storm protection function of these ecosystems has been estimated up to 5 million USD per square kilometer in the United States (Costanza et al., 2008) and 786 million GBP per year for the U.K. marshes (Foster et al., 2013; Goodwin et al., 2018; U.K. National Ecosystem assessment, 2011; Xiaorong et al., 2018). Salt marshes are thought to be relatively stable along the vertical direction, because inorganic matter accumulation and organic mass production allow the marsh to keep pace with sea level; however, salt marshes are seldom in equilibrium along the horizontal direction, and continuously expand or contract in response to external forcing such as wind waves and sediment inputs (e.g., Carniello et al., 2011; Fagherazzi et al., 2013; Leonardi & Fagherazzi, 2014; Leonardi, Defne, et al., 2016; Marani et al., 2011; Schwimmer, 2001; Schwimmer & Pizzuto, 2000). For instance, Schwimmer, 2001 first suggested the existence of a relationship between wave energy and marsh erosion, and then Marani et al., 2011 demonstrated the existence of a linear relation between wave power density and marsh retreat, using a non-dimensional analysis and observations; subsequent studies further corroborated the dependence of marsh erosion and wave power for several locations worldwide (e.g., Leonardi, Ganju, & Fagherazzi, 2016).

Many studies have investigated the feedbacks between vegetation biomass production and marsh elevation (e.g., D'Alpaos et al., 2012; Marani et al., 2007, 2010; Morris et al., 2002). Morris et al. (2002) showed that up to a limit, increasing submergence levels aids the productivity of the salt marsh macrophyte *Spartina alterniflora*. Marani et al., 2007 introduced a 0-D model coupling physical and biological processes and able to reproduce

the different elevations of tidal landforms regularly inundated by the tide and characterized by the presence of different vegetation species; for the different vegetation types, the relationship between biomass change and submergence level was varied depending on the physiological character of the plants. Marani et al. (2010) provided a comprehensive theory to describe stable states and equilibrium shifts in tidal biomorphodynamics and demonstrated that the organic sediment production associated with halophytic vegetation represents a major component of the deposition flux.

Ultimately, the maintenance of salt marsh areal extent has been linked to the sediment budget of the marsh complex as a whole, including not only the vegetated surfaces but also surrounding tidal flats, seabed, and tidal channels (Ganju et al., 2013, 2017). Indeed, Ganju et al. (2017) synthesized sediment budgets of eight microtidal salt marsh complexes and demonstrated the existence of a relationship between sediment budget and the unvegetated-vegetated marsh ratio, indicating that sediment deficits are linked to conversion of vegetated marsh portions to open water.

The regular flooding of marsh surfaces during high tides is one of the most important factors contributing to the delivery of sediments and maintenance of marsh elevation. Among other factors, the frequency and extent of flooding depends on the elevation of the marsh, local tidal range, and dissipative properties of vegetation. Large flooded areas and frequent inundation allow for greater sediment trapping on the marsh platform. Specifically, vegetation stems largely contribute to the accumulation of suspended sediments through two main mechanisms: reduction of flow speed due to increased drag and trapping of sediments within the stems (Knutson et al., 1982; Leonard & Reed, 2002; Möller et al., 1999; Mudd et al., 2010; Yang, 1998). The direct particle capture by stems is strongly dependent on flow velocities and in typical marshes (flow velocity < 0.1 m/s); this contribution makes up less than 10% of the sediment delivered from floodwaters (Mudd et al., 2010).

There have been extensive studies on both vertical and horizontal salt marsh dynamics, and on the response of these ecosystems to changes in hydrodynamics and sediment inputs. However, there is not a specific knowledge about the reverse problem, that is, the impact of marsh loss on tides and sediment budget in coastal embayments (Fortunato & Oliveira, 2005; Friedrichs & Aubrey, 1988; Friedrichs & Madsen, 1992). In this paper we investigate how geomorphic modifications caused by marsh lateral erosion can alter tides and transport dynamics across the whole bay system, and this can in turn affect the survival of marsh ecosystems. Our findings can be applied to a wide range of back-barrier estuaries where salt marshes are located landward and are extremely relevant for coastal communities given that marsh erosion is a common issue. For instance, changes in tidal levels can influence marsh flooding and changes in the sediment budget can alter the resilience of the marsh and of the surrounding coastlines as well.

The Barnegat Bay-Little Egg Harbor system (USA) is used as test case, and a coupled hydrodynamic-sediment transport model is applied. Starting from the current distribution and extent of vegetated marsh areas, different simulations are created, which represent incremental salt marsh loss scenarios. Different erosion scenarios are implemented to quantify changes in hydrodynamics and sediment transport of the whole bay system. We then highlight the influence of salt marsh erosion on the sediment budget of the whole system and discuss the implications in terms of wetland resilience and survival under future sea level rise scenarios.

## 2. Study Site

The Barnegat Bay-Little Egg Harbor estuary (BBLEH) is a shallow lagoon-type estuary located along the east coast of New Jersey, USA, between 39°41'N and 39°56'N latitude and 74°04'W and 74°12'W longitude. The system is composed of three shallow bays: Barnegat Bay, Manahawkin Bay, and Little Egg Harbor, which are separated from the Atlantic Ocean by ~70 km of barrier islands. In the bay the average water depth is 1.5 m, with a maximum of 5 m. The basin has a total surface area of 279 km<sup>2</sup>, and it ranges from 2.0 to 6.5 km in width (Hunchak-Kariouk, 1999). The estuary connects with the ocean through Little Egg Inlet, having a width of approximately 2 km with an average water depth of 10 m, and Barnegat Inlet, which is approximately 400 m wide with an average water depth of 15 m. Tides are primarily semidiurnal, with the M<sub>2</sub> tide being the dominant constituent. The tidal range in the ocean is over 1 m, while within the lagoon the tidal range is significantly attenuated, especially in the north where it reduces to less than 20 cm (Aretxabaleta et al., 2014). As reported by Lathrop and Bogner (2001), natural and human drivers, such as land use change and dredging operations, have drastically reduced salt marsh

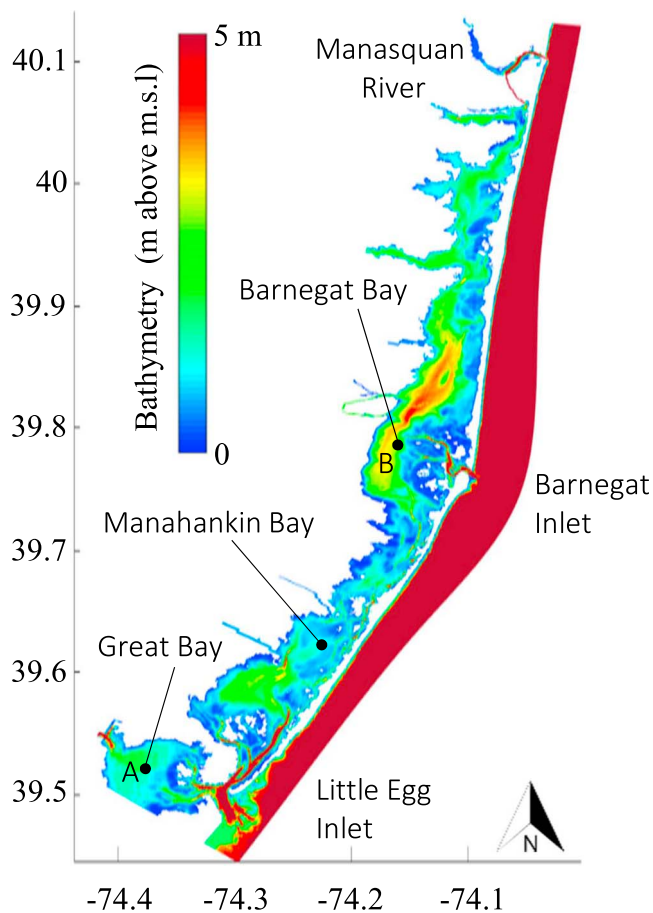


**Figure 1.** Bathymetry of the Barnegat Bay-Little Egg Harbor system.

area from around 14,850 to 9940 ha over the last century. For the majority of the system, salt marsh erosion rates have been relatively constant since the 1930s. Around half of the interior shoreline is eroding less than 0.5 m/year or is not eroding at all; the other half is eroding at around 0.5–2 m/year, and only 2% of the marsh has erosion rates exceeding 2 m/year (Leonardi, Defne, et al., 2016; Leonardi, Ganju, & Fagherazzi, 2016). The highest erosion rates are found in the marshes surrounding Great Bay (Leonardi, Defne, et al., 2016). *Spartina alterniflora* and *Spartina patens* are the dominant species in tidal wetlands of the estuary (Kennish, 2001). The bathymetry of the study area and the distribution of salt marshes are illustrated in Figures 1 and 2a.

### 3. Methods

The Coupled Ocean-Atmosphere-Wave-Sediment Transport (COAWST) modeling framework (Warner et al., 2010) was used to simulate the hydrodynamics and sediment transport processes in the Barnegat Bay-Little Egg Harbor system. The ocean model used in COAWST is ROMS (Regional Ocean Modeling System), which currently incorporates a sediment transport module based on the Community Sediment Transport Modeling System (Shchepetkin & McWilliams, 2005; Warner et al., 2008). The wavefield is simulated by Simulating WAVes Nearshore (Booij et al., 1999). ROMS and Simulating WAVes Nearshore are fully coupled and data exchange occurs every 600 s in this application. The model computes the hydrodynamic flow field, sediment transport, and wind waves on the same computational grid. ROMS solves the finite difference approximations of the Reynolds-averaged Navier-Stokes equations using the hydrostatic and Boussinesq assumptions (Chassignet et al., 2000; Haidvogel et al., 2000) with a split-explicit time stepping algorithm (Haidvogel et al., 2008; Shchepetkin & McWilliams, 2005). The ROMS barotropic and baroclinic time steps are respectively 0.1 and 1 s. Morphology does not adjust dynamically, and changes in estuary geometry are imposed at the beginning of the simulations.

The domain is defined by a numerical grid of dimension  $160 \times 800$  cells with seven layers equally spaced in the vertical. The grid, with cell sizes ranging from 40 to 200 m, was refined around elements with complex geometry and around the inlets. The model is forced at the boundaries of the domain with tides, defined using ADCIRC (Advanced Three-Dimensional Circulation Model) tidal constituents database for the North Atlantic Ocean (Mukai et al., 2002). The calibration of the model was done by changing the bottom roughness coefficient in order to obtain the best accordance with measurements from seven water level stations and three tidal discharge stations within the BBLEH and for a period comprising the first 2 weeks of March 2012. A quadratic drag formulation with a drag coefficient of 0.0015 was used to define the bottom roughness for the whole domain. The modeling framework has been implemented and calibrated by Defne and Ganju (2014). The Brier Skill Score (Murphy & Epstein, 1989) was used to evaluate the model performance, and as reported by Defne and Ganju (2014) skill assessment of the model varies from very good to excellent.

The suspended sediment in the water column is transported by solving the advection-diffusion equation and by accounting for source/sink terms induced by downward settling or upward flux of eroded material. Sediment sources from the bed are computed following Ariathurai and Arulanandan (1978) as  $c_{\text{source}} = \epsilon_s (1 - n) (\tau_w / \tau_c - 1)$  for  $\tau_w > \tau_c$ , where  $\epsilon_s$  is the bed erodibility ( $0.0005 \text{ kg} \cdot \text{m}^{-2} \cdot \text{s}^{-1}$ ),  $n$  is the porosity of the bed (0.5),  $\tau_w$  is the shear stress applied on the bed, and  $\tau_c$  is the critical erosion shear stress of the sediment (0.05 Pa). In our test cases, we only used one class of sediments, having a mass density of  $2,650 \text{ kg} \cdot \text{m}^{-3}$  and a settling velocity of 0.5 mm/s. Values were chosen based on sediment characteristics typical of a coastal embayment (Fagherazzi et al., 2013). Sink terms are calculated as  $c_{\text{sink}} = \partial w_s c / \partial s$ , where  $w_s$  is the vertical settling velocity and the  $s$  coordinate is the vertical sigma coordinate. The friction exerted on the flow by the bed is calculated using the Sherwood-Signell-Warner bottom boundary layer formulation (Warner et al., 2008).

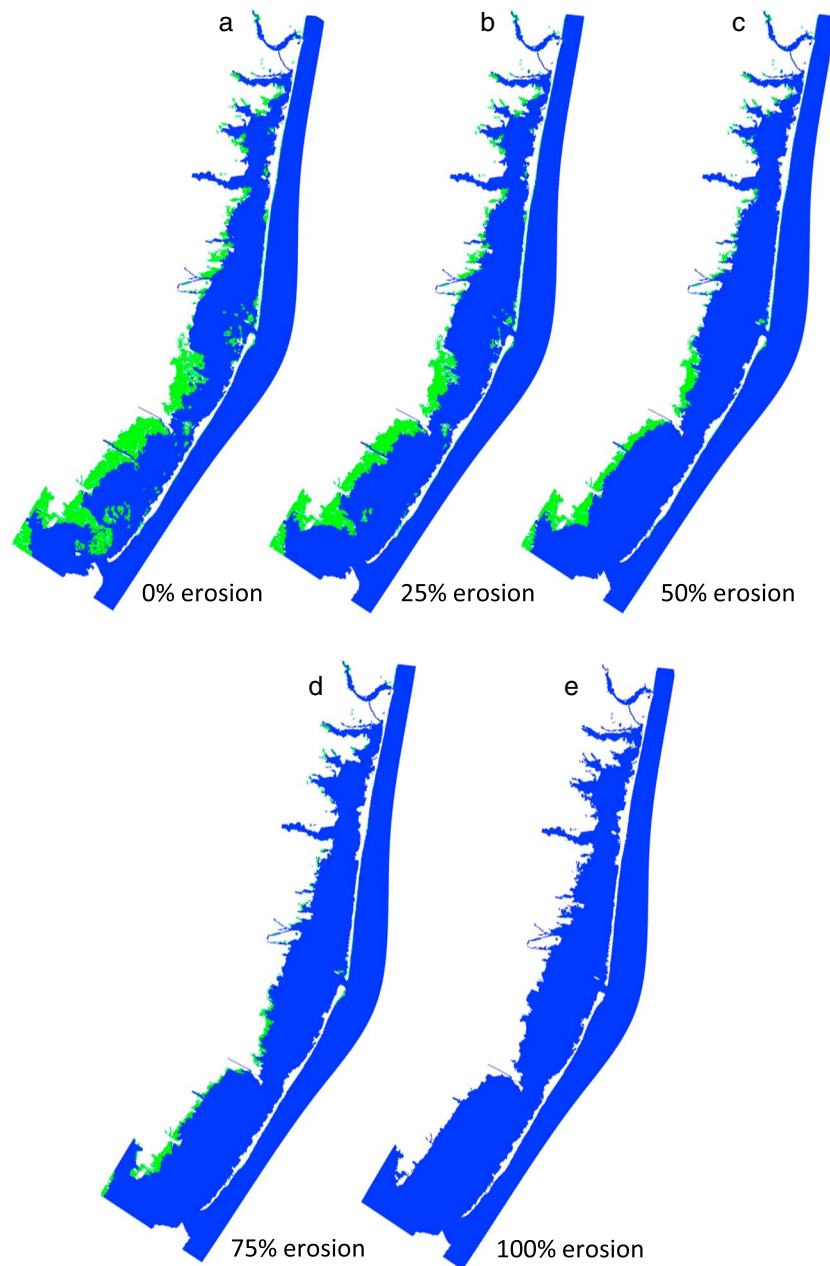


**Figure 2.** Model domains (a–e) under different salt marsh erosion scenarios, that is, BBLEH, BBLEH-25, BBLEH-50, BBLEH-75, and BBLEH-100. Green areas are locations where salt marshes are present. BBLEH = Barnegat Bay-Little Egg Harbor estuary.

The bottom boundary layer roughness is increased by the presence of waves that produce enhanced drag on the mean flow (Ganju & Sherwood, 2010; Madsen, 1994; Styles & Glenn, 2000).

In numerical models, the simplest method to simulate the influence of vegetation on the mean flow is to increase the bottom roughness coefficient (Morin et al., 2000; Ree, 1949). However, this approximation cannot properly represent the three-dimensional influence of vegetation on the mean and turbulent flow (e.g., Lapentina & Sheng, 2014; Marjoribanks et al., 2014). In this paper, a recently implemented vegetation module is used (Beudin et al., 2016). The vegetation module affects the flow field through the plant posture-dependent three-dimensional drag, in-canopy wave-induced streaming, and production of turbulent kinetic energy (Beudin et al., 2016; Kalra et al., 2017). The spatially averaged vegetation drag force is approximated

using a quadratic drag law (equations (1) and (2)), and the effect of plant flexibility on drag is computed using the approach of Luhar and Nepf (equation (3); Luhar & Nepf, 2011):

$$F_{d, \text{veg}, u} = \frac{1}{2} C_D b_v n_v u \sqrt{u^2 + v^2}, \quad (1)$$

$$F_{d, \text{veg}, v} = \frac{1}{2} C_D b_v n_v v \sqrt{u^2 + v^2}, \quad (2)$$

$$\frac{l_{ve}}{l_v} = 1 - \frac{1 - 0.9Ca^{-1/3}}{1 + Ca^{-3/2}(8 + B^{3/2})}, \quad (3)$$

where  $C_D$  is the plant drag coefficient,  $b_v$  is the width of individual plants,  $n_v$  is the number of plants per unit area,  $(u, v)$  are the horizontal velocity components at each vertical layer,  $Ca$  is the Cauchy number,  $B$  is the buoyancy parameter, and  $l_{ve}$  is the length of a rigid vertical blade that generates the same drag on the mean flow as a flexible cylinder of length  $l_v$ .

Apart from the mean flow velocity, vegetation also significantly impacts turbulence intensity and mixing. The selected turbulence model is the  $k-\epsilon$  scheme (Rodi, 1984), which accounts for extra dissipation and turbulence kinetic energy production due to vegetation (Uittenbogaard, 2003). Turbulence influences settling velocities of particles and a reduction in turbulent energy can lead to enhanced particle settling in salt marshes (e.g., Christiansen et al., 2000; Leonard & Croft, 2006; Leonard & Luther, 1995; Nepf, 1999).

In this work, we used uniform values of canopy structure and density; however, these parameters can vary widely in tidal marshes. In the model, plant stems are 50 cm high, 0.1 cm wide, with 1-mm thickness, and the stem density is defined as 250 stems per square meter (U.S. Department of Agriculture, 2008). The mass density and elastic modulus are equal to 700 kg/m<sup>3</sup> and 1 kN/mm<sup>2</sup>, respectively (Feagin et al., 2011), the drag coefficient is set to 1. The marsh coverage data came from the Center for Remote Sensing and Spatial Analysis's geographic information systems database. Different salt marsh loss scenarios are tested, which represent a uniform erosion of the marsh areas (Figure 2); these are simplified cases as some marshes within the bay eroded faster than others (Leonardi, Defne, et al., 2016; Leonardi, Ganju, & Fagherazzi, 2016). Loss percentage ranges from 25% to 100% (when all vegetated areas are removed). Results are presented in terms of marsh loss percentages. The erosion of salt marshes was simulated by removing vegetation from the eroded marsh cells and by matching the corresponding bathymetry values with the elevation of the surrounding tidal flats. For each vegetated pixels was checked whether one of the bordering elements was water. If one of the bordering element was water, the marsh pixel was transformed into water by assigning as bathymetry value the average of the elevations of the nearby water pixels. The algorithm was repeated enough time to reach a reduction of 25%, 50%, 75%, and 100%.

As marsh erosion is associated with an increase in tidal prism the size of the inlets has been updated following the O'Brien-Jarrett-Marchi law (D'Alpaos et al., 2010; FitzGerald, 1996; FitzGerald et al., 2004, 2008; Jarrett, 1976; List et al., 1994, 1997; O'Brien, 1931, 1969), (Figure 2). Specifically, we calculated the slope coefficient of the O'Brien-Jarrett-Marchi law with an exponent equals to 6/7 for the existing configuration, and we modified the cross-sectional area by increasing only the width of the inlets.

For those simulations used to investigate the transport of sediments, a spatially uniform concentration value is imposed at the starting time in areas inside the bay system. Specifically, the sediment injection occurs at mean sea level and during the first flood period. During the simulation there are no other external sediments inputs. Morphological updates, as well as depositional and erosional fluxes, only account for those sediments that are placed in suspension at the simulation start time.

Several scenarios are simulated to evaluate the effects of marsh erosion on the hydrodynamics and sediment budget of the system. Basic scenarios are summarized into Table 1: (1) BBLEH: current salt marsh distribution (no erosion); (2) BBLEH-25: 25% of salt marshes are eroded; (3) BBLEH-50: 50% of salt marshes are eroded; (4) BBLEH-75: 75% of salt marshes are eroded; (5) BBLEH-100: Salt marshes are completely eroded; (6) vegetation die-off: Vegetation is completely removed, but there are no morphological changes with respect to the 0% erosion case. All the simulations are forced at the open boundaries by tidal forcing, defined using nine constituents:  $K_1$ ,  $O_1$ ,  $Q_1$ ,  $M_2$ ,  $S_2$ ,  $N_2$ ,  $K_2$ ,  $M_4$ , and  $M_6$ . In addition, we test the



**Table 1**  
List of Numerical Runs

Model scenario	Marsh loss	Forcings
BBLEH	0%	Tides, Tides + Waves
BBLEH-25	25%	Tides
BBLEH-50	50%	Tides
BBLEH-75	75%	Tides
BBLEH-100	100%	Tides, Tides + Waves
Vegetation die-off	0%	Tides
BBLEH-M <sub>2</sub>	0%	M <sub>2</sub> tidal component
BBLEH-0.95-M <sub>2</sub>	0%	0.95 M <sub>2</sub> tidal component
BBLEH-0.90-M <sub>2</sub>	0%	0.90 M <sub>2</sub> tidal component
BBLEH-0.85-M <sub>2</sub>	0%	0.85 M <sub>2</sub> tidal component
BBLEH-0.80-M <sub>2</sub>	0%	0.80 M <sub>2</sub> tidal component
BBLEH-25-M <sub>2</sub>	25%	M <sub>2</sub> tidal component
BBLEH-50-M <sub>2</sub>	50%	M <sub>2</sub> tidal component
BBLEH-75-M <sub>2</sub>	75%	M <sub>2</sub> tidal component
BBLEH-100-M <sub>2</sub>	100%	M <sub>2</sub> tidal component

Note. BBLEH = Barnegat Bay-Little Egg Harbor estuary.

effects of locally generated waves for the scenario with the current salt marsh distribution (BBLEH) and the scenario with the removal of the entire marsh surface (BBLEH-100). For these test cases a constant south-west wind of 10 m/s is assumed. Barnegat Bay is mostly influenced by locally generated waves and given the orientation of the bay, the south-west direction is the one corresponding to the highest fetch values (Figure S5a in the supporting information).

Throughout the manuscript we will show that changes in marsh areal extent modify tidal amplitudes. To unravel whether the associated changes in sediment balance are mainly impacted by the sole reduction of marsh areal extent or by the sole changes in tidal amplitude, a set of idealized simulations are conducted. Five simulations are forced by the main tidal component (M<sub>2</sub>) for different marsh erosion scenarios (0%, 25%, 50%, 75%, and 100%). Five additional simulations have a constant marsh area (0% erosion case) but are forced at the boundary through an M<sub>2</sub> harmonic reduced by 0%, 5%, 10%, 15%, and 20% with respect to existing values (Table 1).

## 4. Results

The first two sections deal with hydrodynamic results with a special focus on changes in tidal prism and tidal amplitude as a consequence of salt marsh loss. In the third part we investigate the influence of salt marsh loss on the sediment trapping potential and sediment budget of the bay.

### 4.1. Influence of Salt Marsh Loss on Tidal Prism

The tidal prism value,  $P$ , was assessed at spring tide as the volume entering the bay between high and low tides. The tidal prism increases as a consequence of salt marsh loss (Figure 3). The percentage increase in tidal prism correlates well with the increment in basin area ( $R^2 = 0.99$ ), and a polynomial fit was used to highlight the nonlinear behavior of the system.

The fact that the relationship presented in Figure 3 differs from a straight line with a unit slope suggests that variations in tidal prism associated with an increase in basin area are also accompanied by changes in tidal amplitude. Indeed, the tidal amplitude within the bay considerably decreases once the marsh is eroded as shown by a comparison of the time series of water levels for two points located in the center of Great Bay

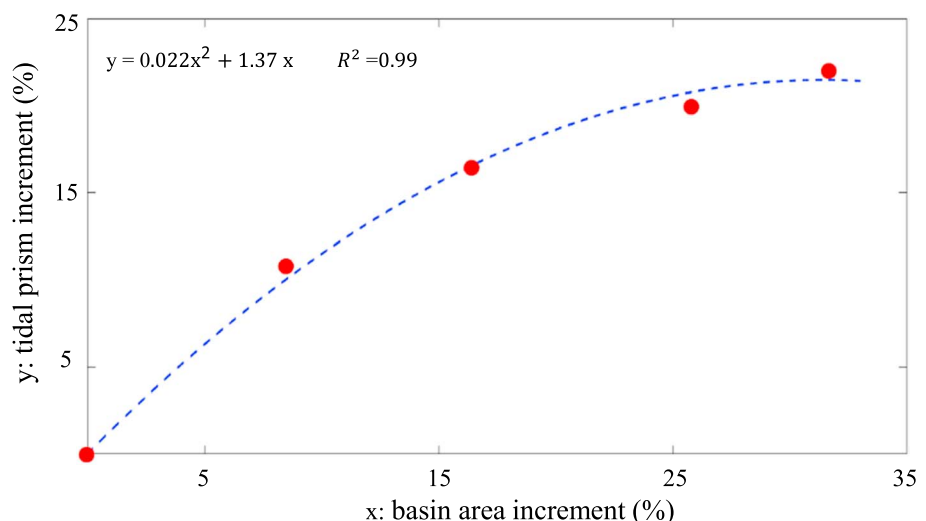


**Figure 3.** Relationship between percent increment in tidal prism and percentage increment in basin area with salt marsh loss.

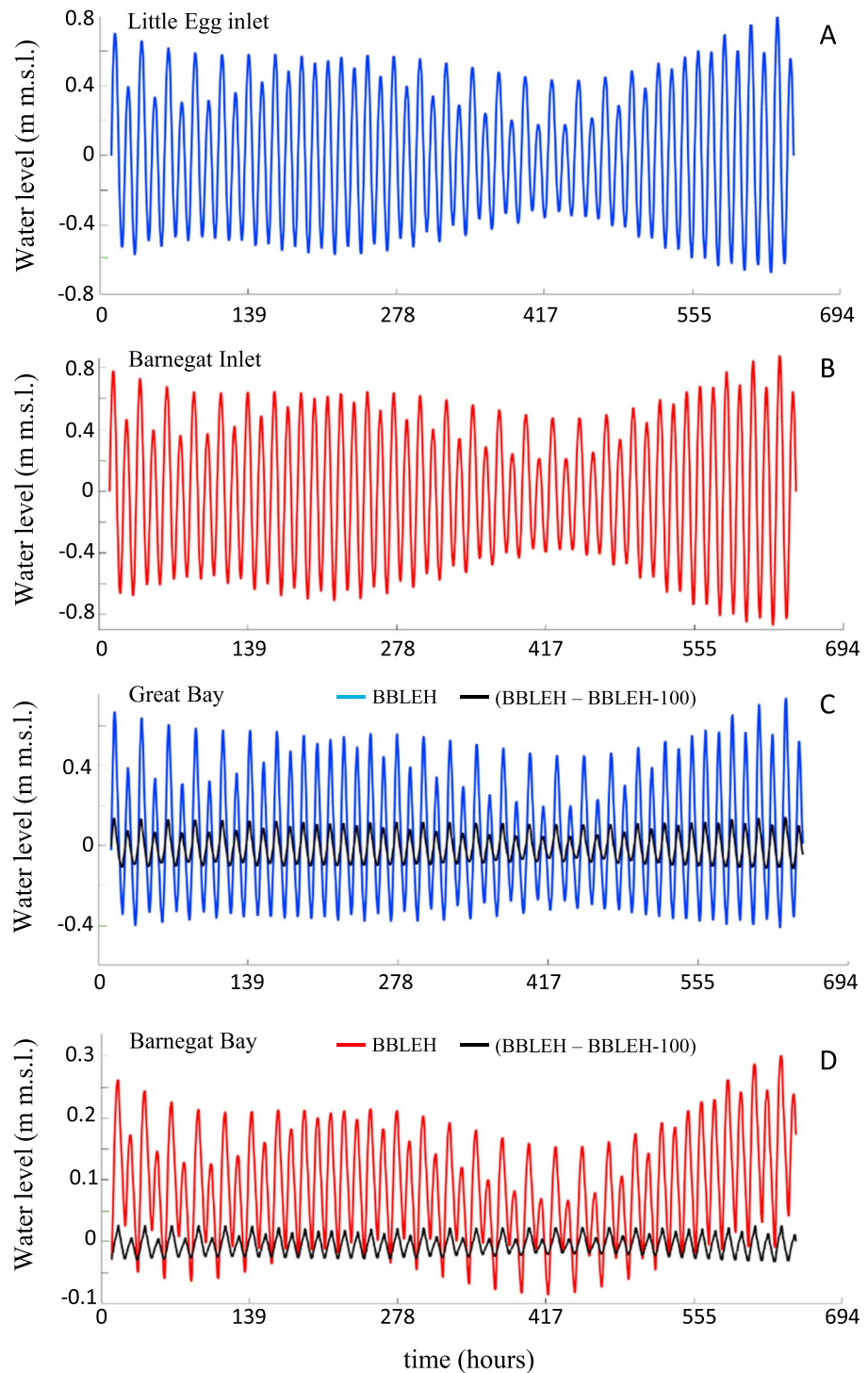


**Figure 4.** Time series of water levels at Little Egg Inlet (a) and Barnegat Inlet (b); time series of water levels for one point in Great Bay (point A, Figure 1a) and in Barnegat Bay (point B, Figure 1a). Colored lines represent water level fluctuations for the scenario with the current salt marsh configuration, while black lines represent differences in water level fluctuations between the 0% and 100% erosion scenarios. BBLEH = Barnegat Bay-Little Egg Harbor estuary.

and Barnegat Bay (points A and B, Figures 1a, 4c, and 4d); colored lines are water levels for the 0% marsh erosion case, and black lines are the difference in water level before and after the removal of the marsh. The water levels at the inlet sections are presented in Figures 4a and 4b.

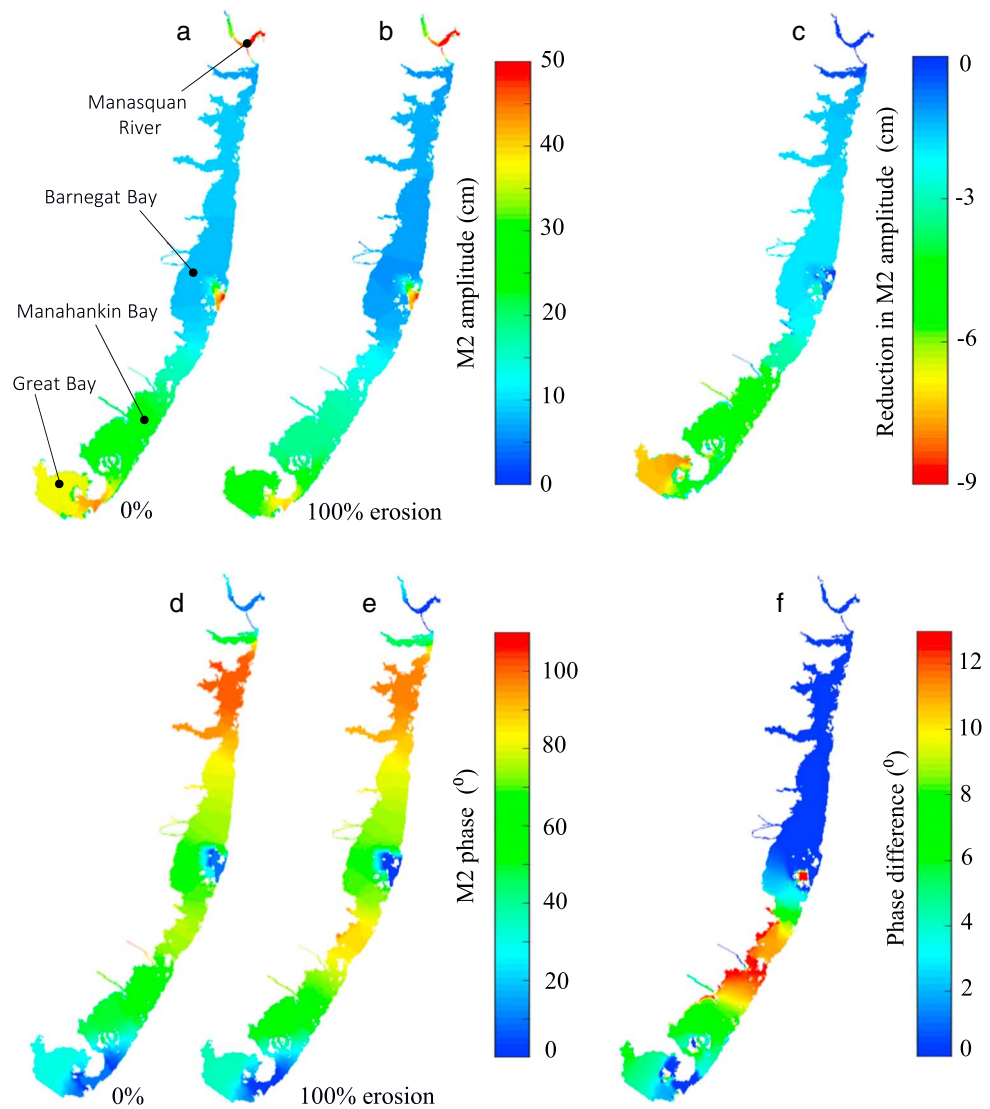


**Figure 5.** (a)  $M_2$  amplitude (cm), for the 0% erosion case. (b)  $M_2$  amplitude (cm) after removal of the entire marsh surface, 100% erosion scenario. (c) Difference in  $M_2$  amplitude (cm) between the case with salt marshes completely eroded and the case with the current salt marsh extent. (d)  $M_2$  phase lag in Barnegat Bay-Little Egg Harbor estuary; (e)  $M_2$  phase lag after removal of the entire marsh surface. (f) Difference in phase lag between the case with salt marshes completely eroded and the case with the current salt marsh extent.

#### 4.2. Influence of Salt Marsh Loss on Tidal Propagation Within the Bay

For a shallow bay characterized by a complex geometry, significant variations in the tidal signal are expected across different portions of the domain, as well as between spring and neap tides. We computed the spatial distribution of the amplitude and phase lag of the  $M_2$  constituent using T\_Tide (Pawlowicz et al., 2002); this harmonic has most of the tidal energy and can be considered representative of the tidal signal of the system.

The tidal signal within the bay is strongly damped with respect to the ocean boundary, which is in agreement with previous investigations (e.g., Aretxabaleta et al., 2014). The smallest tidal amplitude is observed in Barnegat Bay, due to the smaller cross section of Barnegat Inlet with respect to Little Egg Inlet (Figure 5a). The tidal signal in the bay is also delayed with respect to the tide in the ocean. (Figure 5d). The phase shift is maximum in Barnegat Bay whose far end has a delay of  $110^\circ$  (3.5 hr). Little phase shift is noticeable in Great Bay and in the Manasquan River.



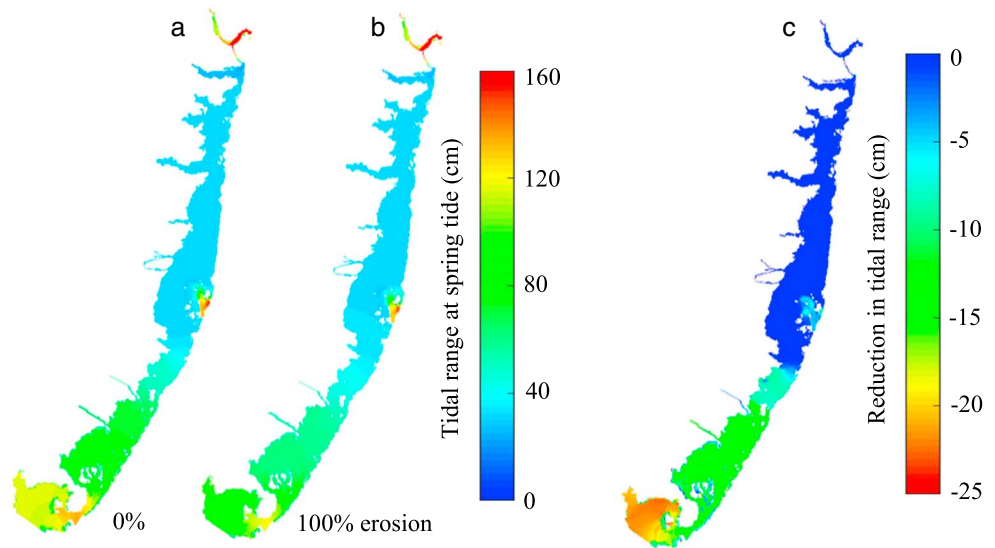


**Figure 6.** Tidal range (cm) in spring tide conditions. (a) For the current salt marsh extent. (b) After removal of the entire marsh surface. (c) Difference in tidal range between the case with salt marsh completely eroded and the case with the current salt marsh distribution.

A comparison between amplitude and phase lag values for the current salt marsh configuration, and after the complete erosion of the marsh (Figures 5b and 5e), reveals that the entire domain experiences a decrease in amplitude and an increase in phase lag once the marsh is completely eliminated from the system (Figures 5c and 5f). Changes in  $M_2$  amplitude vary from 0 to 9 cm, with the highest reduction occurring in Great Bay whose geometry changes the most after removal of vegetated areas (Figures 1 and 2). In terms of phase lag, Great Bay and Manahankin Bay are the areas experiencing the largest changes, getting a maximum increment of the phase lag of  $13^\circ$  (about 27 min). This outcome is confirmed when considering changes in spring (Figure 6) and neap tide (Figure 7) as consequence of salt marsh erosion; the spatial distribution of differences in tidal amplitude is similar to the one of the  $M_2$  component.

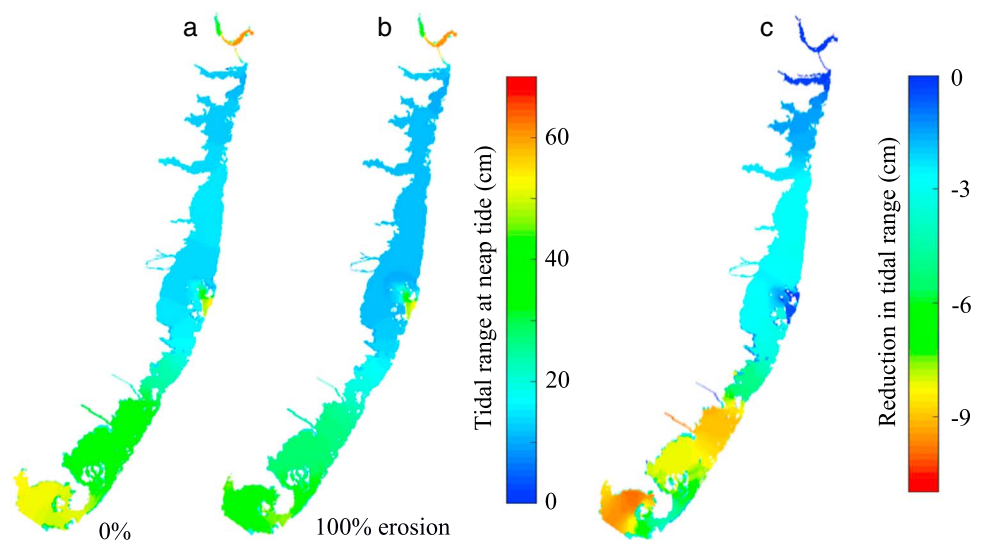


**Figure 7.** Tidal range (cm) in neap tide conditions. (a) For the current salt marsh distribution. (b) After the removal of the entire marsh surface. (c) Difference in tidal range between the case with salt marsh completely eroded and the case with the current salt marsh distribution.

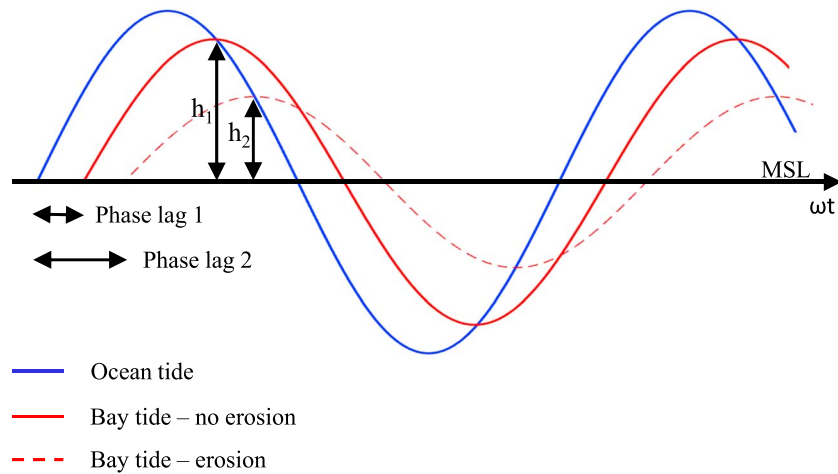


**Figure 8.** Time histories of idealized ocean and bay tides. MSL = mean sea level.

The erosion of the marsh changes the morphology of the bay, which in turn causes interrelated variations of phase lag and tidal amplitude. Indeed, as the phase lag between the ocean and the lagoon wave increases, the standing character of the tidal wave declines, leading to a reduction in the magnitude of the signal within the system. Figure 8 illustrates an idealized time history of tides in the ocean and in the bay. As the water level in the ocean is higher than the bay level, a flow is generated at the inlet, which fills and raises the water level within the bay. When the high tide is reached in the ocean, the water level in the bay keeps rising due to existing phase lag values, and the bay continues to fill until the water level in the ocean and the one in the bay are the same. When the marsh is eroded a slower increase in water levels within the bay caused by an increase in the intertidal storage volume delays the tidal wave and increases the phase lag. An increment in phase lag causes maximum water level values within the bay to decrease as the peak of the tidal wave occurs later in the falling limb of the ocean wave (Keulegan, 1967). For the BBLEH the hydrodynamics of the problem is significantly more complicated with respect to the idealized diagram in Figure 8, as rather than having a single-inlet system, there are two inlets and therefore two overlapping waves entering the bay (Aretxabaleta et al., 2017). As the amplitude and phase of the main tidal constituent change with the increase of the intertidal storage volume, tidal asymmetry should also be affected by marsh lateral erosion. Changes in the  $M_4$  to  $M_2$  sea surface amplitude ratio and the sea surface phase  $M_4$  relative to  $M_2$  were calculated following Aubrey and Speer (1985). The amplitude and phase ratios of the system with the current salt marsh distribution and with marshes completely eroded are depicted in Figure 9. The magnitude of the nonlinear distortion increases (+15% on average) when marshes retreat (Figures 9a and 9b) and although the relative phase moves away from the limit that would provide maximum asymmetry, the estuary remains flood dominant ( $0^\circ < \varphi < 180^\circ$ , Figures 9b and 9d; Araújo et al., 2008; Friedrichs & Aubrey, 1988; Picado et al., 2010). The average of the maximum shear stress calculated during a spring tidal cycle increases around 5% during the ebb phase and 7% during the flood phase with marsh loss.

Extensive vegetation die-off without erosion (i.e., same morphology than Figure 2a but no vegetation, Figure S1a) does not significantly impact the tidal propagation within the bay. Vegetation die-off still influences tidal propagation and energy dissipation over the marsh platforms. This result is connected to the fact that fringing marshes are at the boundary with the mainland and different results might be expected for salt marshes located at the center of the embayment or for different vegetated surfaces such as seagrasses (e.g., Donatelli et al., 2018). A comparison between the amplitude of the main harmonic with and without full vegetation cover of the marsh platform shows that changes in the frictional character of marsh platforms do not impact the tidal propagation into the back-barrier basin (Figures S1b and S1c) but influences the propagation of the tide on marsh platforms by reducing the flooded areas by 15% (Figure S1d).

#### 4.3. Influence of Salt Marsh Loss on the Sediment Trapping Potential of Shallow Bays

The stability of coastal wetlands and their survival in response to sea level rise and external forcing depends on the sediment budget of the system (e.g., Fagherazzi et al., 2013; Ganju et al., 2013, 2017). As shown in the

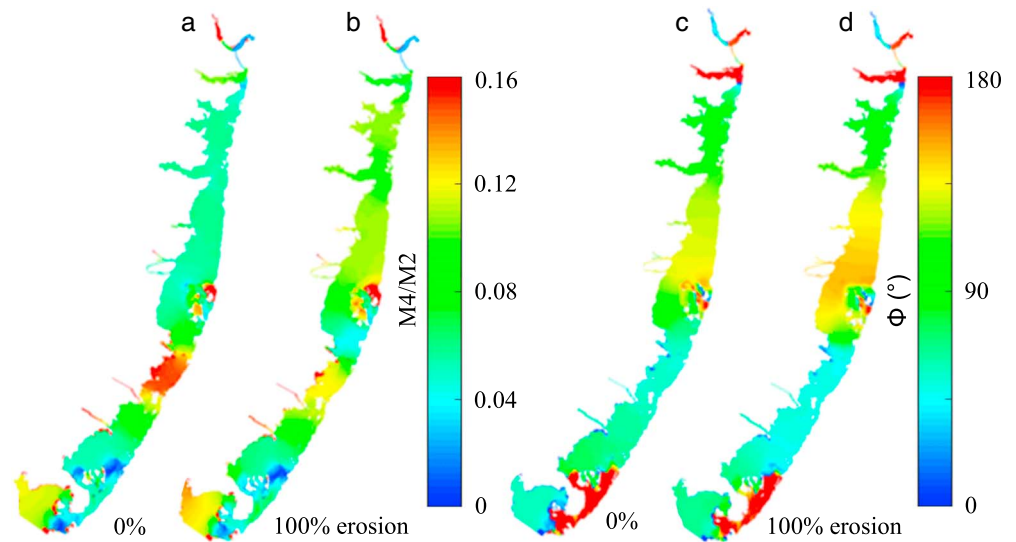


**Figure 9.** (a) Sea surface amplitude ratio for the current marsh distribution and (b) marsh completely eroded. (c) Sea surface phase of  $M_4$  relative to  $M_2$  for the current marsh distribution and (d) marsh completely eroded.

previous section, salt marsh erosion increases the tidal prism, which could in turn enhance the flushing capacity of the system and distort the tidal signal causing thus a possible increase in the loss of sediments during a tidal cycle and a reduction in the sediment-trapping capability of the bay. Furthermore, a reduction in tidal amplitude can decrease plant biomass production (Morris et al., 2002).

To test this hypothesis, and to investigate the sediment trapping potential of salt marshes, we conducted a series of experiments focusing on sediment dynamics. For every salt marsh loss scenario, a 30-day simulation was run by superimposing at  $t = 0$ , and over the initial footprint of the lagoon open-water area, a uniform (100 mg/L) suspended sediment concentration. The sediment injection occurs instantaneously at mean sea level and at the beginning of the simulation, during the first flood phase. The sediment injection occurs only once. The initial suspended sediment mass is equal for each erosion scenario because the footprint where the initial sediment concentration is imposed is the same. A uniformly distributed input sediment concentration represents potential riverine inputs during flood conditions or large resuspension events during storms; such conditions represent major contributors of inorganic sediments to salt marshes (e.g., Fagherazzi & Priestas, 2010; Falcini et al., 2012; Leonardi et al., 2017). A qualitative assessment about the order of magnitude of suspended sediment concentration values is presented in Table S1 and Figure S2.

Sediments can be stored within the estuary in one of the following forms, which are quantified for the different erosion scenarios: (i) Suspended sediment in the water column, (ii) sediment deposited on tidal flats and over the within-bay seabed, and (iii) sediment deposited within the vegetated areas. The sum of these quantities represents the total mass of sediments within the bay, and it tends to decline in time because some sediments are flushed out of the bay system during ebb (Figure S4). The total mass of sediments stored within the bay exponentially decays and asymptotically approaches equilibrium values. Specifically, given the existing marsh configuration (0% erosion), equilibrium values are approached after 5 days, while it takes 18 days for the system to reach equilibrium when the marsh is completely removed (100% erosion; Figure S4).

When the salt marsh is removed, the total amount of sediments stored within the lagoon largely decreases (Figures 8 and S4). Figure 9 illustrates how marsh loss alters the eventual destination of deposited sediment mass. The sediment mass deposited on tidal flats and the seabed (Figure 11a) linearly decreases when the marsh is eroded. The suspended sediment mass tends instead to increase with increasing marsh loss (Figure 11b). The sediment mass trapped by vegetation (Figure 11c) and deposited on vegetated marsh areas exponentially decreases when marsh is lost. This is due to two main mechanisms: (i) from a geometrical point of view, the spatial extent covered by vegetation where sediments can

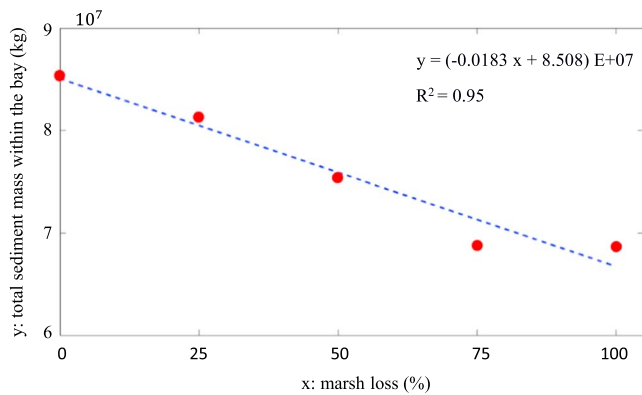


**Figure 10.** Total sediment mass stored in the domain as a function of percentage increment in marsh loss and after 30 simulated days.

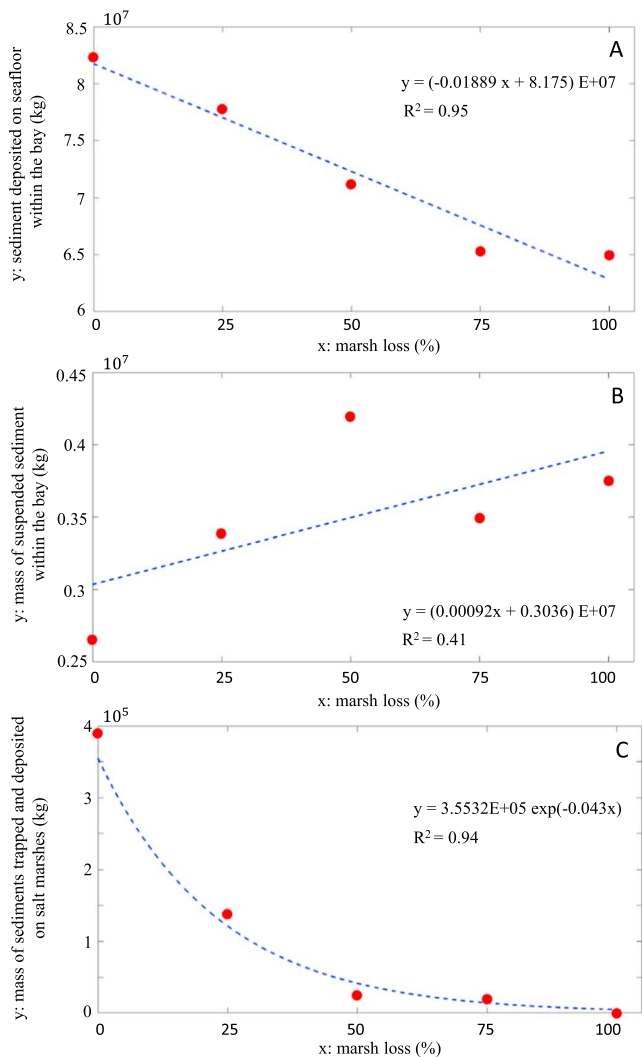


**Figure 11.** (a) Mass of sediments deposited on tidal flats and on the *within-bay* bed. (b) Mass of sediments in suspension. (c) Mass of sediments trapped and deposited on the vegetated marsh, as a function of percentage increment in marsh loss and after 30 simulated days.

deposit decreases when the salt marsh erodes and (ii) increasing marsh loss reduces tidal amplitudes and the submergence level of the marsh. The exponential decrease indicates that the removal of 25% of the marsh area causes a reduction in the sediment mass trapped by the marsh of more than 50% and that a removal of 50% of the marsh has an effect comparable to the removal of the entire vegetated surface.

When waves are added to the model the associated increase in bottom shear stress causes greater sediment resuspension; this leads to a large increase in the sediment mass deposited on marsh platforms and a decrease in tidal flat deposits. Generally, the presence of waves decreases the total sediment mass stored within the bay (Figure S5b). Overall trends in sediment storage in response to salt marsh removal in the presence of waves are the same than for cases without waves (Figure S6).

For the sediment storage on marsh platforms, to test the relative importance of the direct impact associated to a reduction of salt marsh area extent with respect to the indirect impact related to the erosion-induced decrease in tidal amplitude, we conducted a set of idealized simulations. Given the same bay morphology (0% erosion scenario), different scenarios were forced at the ocean boundary by  $M_2$  signals with varying amplitude (Figure S7a). Specifically, tested values for the  $M_2$  component ranged from the existing 0.59 to 0.47 m, with the latter being a 20% reduced value in agreement with the average within-bay decrease in tidal amplitude associated to the 100% erosion case. Different erosion scenarios were then tested, which were forced by the sole  $M_2$  component (Figure S7b). We estimate that a 20% reduction in tidal amplitude reduces the sediment trapping on marsh platform by 30%.

### 5. Discussions

Salt marsh losses have been documented worldwide because of land use change, wave erosion, and sea level rise. Using the COAWST modeling framework, the impact of salt marsh erosion on the tidal propagation and sediment budget of a shallow lagoon-type estuary has been studied.

Salt marsh loss causes an increase in tidal prism and a decrease in the sediment trapping capacity of the lagoon system (Figure 10). Salt marsh erosion also decreases tidal amplitude values across the entire domain (Figures 4–7). The areas subject to the highest variations in tidal amplitude are the ones where geometric variations associated to marsh loss are more pronounced. Changes in tidal amplitude are due to the increased filling time of the system and to the consequent increase in phase lag between the ocean and bay-tidal signals.

Our results show that an increase in the intertidal storage volume dampens the tidal wave for those systems where the increased filling time is the main consequence associated to marsh erosion.

Specifically, we have shown that when marshes are located landward, marsh lateral erosion can induce changes in tidal dynamics that could lead to a positive feedback, which is detrimental for marsh survival (i.e., lower amplitude, less biomass production, and lower vertical growth).

Our findings are in agreement with studies carried out in the coastal lagoon Ria de Aveiro, Portugal (Picado et al., 2010). For the coastal lagoon Ria de Aveiro, the authors showed how the enlargement of the lagoon

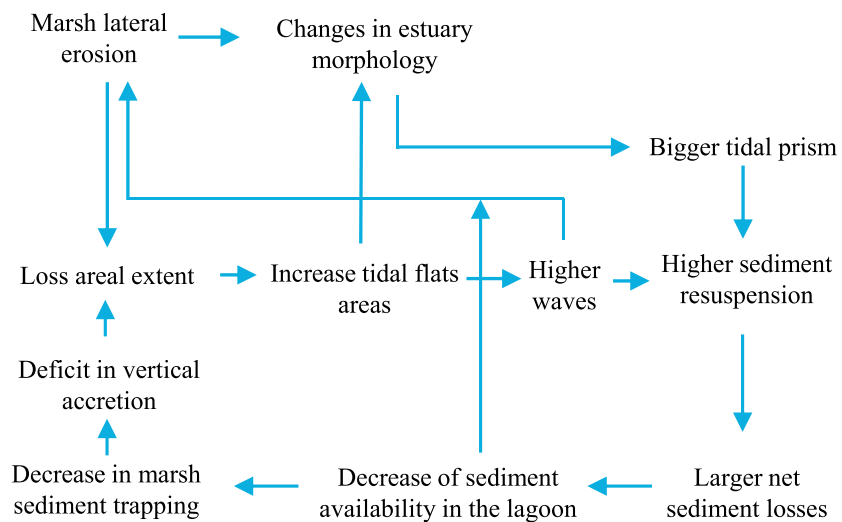


**Figure 12.** Feedbacks between salt marsh lateral erosion and marsh sediment trapping reduction.

flooded area, due to the collapse of protective walls, decreases tidal amplitude within the system. With respect to Barnegat Bay, Ria de Aveiro has a different number of inlets (number of inlets = 1), different tidal range (2 m), and different geometry.

The findings have been verified for shallow lagoon-type estuaries and marshes fringing the landward side of the estuary; different results might occur when salt marshes are located at the center of the embayment or at seaward side of the embayment, or in case of estuaries with very different morphologies, for example, significantly longer and deeper estuarine channels.

Salt marsh lateral erosion enhances the export of sediments and reduces the sediment delivery to marsh platforms and the storage of sediments on tidal flats (Figure 11). Such changes in the sediment budget could trigger a positive feedback undermining salt marsh survival to climate change: Once the marsh is eroded, the capability of the system to store sediments declines and sediments are more easily lost in the open ocean; accretion rates are also reduced as the marsh platform receives less sediments during inundation periods. A reduction in the sediment mass available in the estuary affects negatively marsh stability, because without an adequate sediment supply, vegetated areas are more easily converted into open water (Ganju et al., 2017). Furthermore, an increase in tidal flat areas increases the erosion hazard connected to locally generated waves, which could more easily develop; finally, a reduction in salt marsh accretion rates could cause salt marshes to be more susceptible to sea level rise as a consequence of which a further increase in tidal prism and accelerated marsh submergence rates might occur (Figure 12). A shortcoming of this modeling framework is related to the usage of only one sediment fraction and to the choice to remove all of the sediments deriving from the progressive reduction in salt marsh area. In reality, the erosion of marsh edges generates a source of sediments, which can be delivered to the marsh trough channels or be directly dropped on submerged marsh platform. This sediment could contribute to salt marsh survival and affect the geomorphological evolution of the bay over long time scales. This approach would cause an overestimation of marsh vulnerability if the morphological evolution of the marsh was explicitly accounted for. However, while possibly underestimating the absolute mass of sediments available within the embayment, this approach does not undermine the main outcome concerning the reduction of the potential sediment storage capability of shallow bays as a consequence of salt marsh erosion.

## 6. Conclusions

Many studies have focused on the impact of external agents on marsh ecosystems, and much focus has been rightly given to the understanding of how climate change might impact salt marshes. However, the reverse problem, that is, how the morphological changes of salt marshes, possibly associated to climate change, are influencing the hydrodynamic and sediment transport of large-scale coastal environments is still poorly



understood. This contribution focuses on the influence of salt marsh erosion on tidal fluctuations, and sediment trapping potential of shallow bays and associated consequences in terms of system vulnerability. The Barnegat Bay-Little Harbor system, a lagoon-type estuary located along the east coast of United States is used as a test case.

Salt marsh erosion influences the sediment budget of bay systems, and for our case study salt marsh loss has been found to largely decrease the capability of the bay to retain sediments. The amount of sediments stored within the bay has been classified into three classes: average suspended sediments in the water column, sediments deposited on tidal flats and on the within-bay seabed, and sediments deposited on vegetated surfaces. The amount of sediments trapped on the vegetated surfaces decreases exponentially with the conversion of the system to open water, and in our test case a 50% removal of the marsh surface has an effect comparable to the complete removal of the marsh (Figure 9c). This decline is connected to two mechanisms: (i) a direct impact associated to the decrease in the spatial extent of vegetated areas where deposition is possible and (ii) an indirect impact connected to the decrease in tidal amplitude and associated reduced delivery to marsh platforms; the latter has been found to be less important in marsh sediment trapping. The amount of sediments deposited on tidal flats shows a linear decrease with salt marsh lateral erosion. Generally, as the marshes erode, the capability of the system to retain sediments decreases; therefore, positive feedbacks between marsh erosion and a decrease in the available sediment could be triggered, which is detrimental for salt marsh survival and especially for the maintenance of vertical accretion rates.

#### Acknowledgments

Data are available in the following repositories: Donatelli (2018a) to Donatelli (2018s). We thank the editor, the AE, the reviewers, and Alfredo Aretxabaleta for critical revision of the manuscript. This work was funded by the Department of the Interior/U.S. Geological Survey award ID G16AC00455.

#### References

- Allen, J. R. L., & Pye, K. (1992). *Saltmarshes: Morphodynamics, conservation, and engineering significance* (p. 196). Press, U. K.: Cambridge University.
- Araújo, I. B., Dias, J. M., & Pugh, D. T. (2008). Model simulations of tidal changes in a coastal lagoon, the Ria de Aveiro (Portugal). *Continental Shelf Research*, 28(8), 1010–1025. <https://doi.org/10.1016/j.csr.2008.02.001>
- Aretxabaleta, A. L., Butman, B., & Ganju, N. K. (2014). Water level response in back-barrier bays unchanged following Hurricane Sandy. *Geophysical Research Letters*, 41, 3163–3171. <https://doi.org/10.1002/2014GL059957>
- Aretxabaleta, A. L., Ganju, N. K., Butman, B., & Signell, R. P. (2017). Observations and a linear model of water level in an interconnected inlet-bay system. *Journal of Geophysical Research: Oceans*, 122, 2760–2780. <https://doi.org/10.1002/2016JC012318>
- Ariathurai, C. R., & Arulanandan, K. (1978). Erosion rates of cohesive soils. *Journal of the Hydraulics Division*, 104(2), 279–282.
- Aubrey, D. G., & Speer, P. E. (1985). A study of non-linear tidal propagation in shallow inlet estuarine systems. Part I. Observations. *Estuarine, Coastal and Shelf Science*, 21(2), 185–205. [https://doi.org/10.1016/0272-7714\(85\)90096-4](https://doi.org/10.1016/0272-7714(85)90096-4)
- Beudin, A., Kalra, T. S., Ganju, N. K., & Warner, J. C. (2016). Development of a coupled wave-flow vegetation interaction model. *Computers & Geosciences*, 100, 76–86.
- Booij, N., Ris, R. C., & Holthuijsen, L. H. (1999). A third-generation wave model for coastal regions, part I, model description and validation. *Journal of Geophysical Research*, C4, 7649–7666. <https://doi.org/10.1029/98JC02622>
- Boorman, L. A. (1995). Sea level rise and the future of the British coast. *Coastal Zone Topics: Process, Ecology and Management*, 1, 10–13.
- Carniello, L., D'Alpaos, A., & Defina, A. (2011). Modeling wind waves and tidal flows in shallow micro-tidal basins. *Estuarine, Coastal and Shelf Science*, 92(2), 263–276. <https://doi.org/10.1016/j.ecss.2011.01.001>
- Chassignet, E. P., Arango, H. G., Dietrich, D., Ezer, T., Ghil, M., Haidvogel, D. B., et al. (2000). DAMEE-NAB: The base experiments. *Dynamics of Atmospheres and Oceans*, 32(3–4), 155–183. [https://doi.org/10.1016/S0377-0265\(00\)00046-4](https://doi.org/10.1016/S0377-0265(00)00046-4)
- Christiansen, T., Wiberg, P. L., & Milligan, T. G. (2000). Flow and sediment transport on a tidal salt marsh surface. *Estuarine, Coastal and Shelf Science*, 50(3), 315–331. <https://doi.org/10.1006/ecss.2000.0548>
- Costanza, R., d'Arge, R., de Groot, R., Farber, S., Grasso, M., Hannon, B., et al. (1997). The value of the world's ecosystem services and natural capital. *Nature*, 387(6630), 253–260.
- Costanza, R., Perez-Maqueo, O., Martinez, M. L., Sutton, P., Anderson, S. J., & Mulder, K. (2008). The value of coastal wetlands for hurricane protection. *Ambio*, 37(4), 241–248. [https://doi.org/10.1579/0044-7447\(2008\)37\[241:TVOCWF\]2.0.CO;2](https://doi.org/10.1579/0044-7447(2008)37[241:TVOCWF]2.0.CO;2)
- D'alpaos, A., Da Lio, C., & Marani, M. (2012). Biogeomorphology of tidal landforms: Physical and biological processes shaping the tidal landscape. *Ecology*, 93(5), 550–562. <https://doi.org/10.1002/eco.279>
- D'Alpaos, A., Lanzoni, S., Marani, M., & Rinaldo, A. (2010). On the tidal prism–channel area relations. *Journal of Geophysical Research*, 115, F01003. <https://doi.org/10.1029/2008JF001243>
- Defne, Z., & Ganju, N. (2014). Quantifying the residence time and flushing characteristics of a shallow, back-barrier estuary: Application of hydrodynamic and particle tracking models. *Estuaries and Coasts*, 1–16. <https://doi.org/10.1007/s12237-014-9885-3>
- Donatelli, C. (2018a). bbleh. <https://doi.org/10.5281/zenodo.1210164>
- Donatelli, C. (2018b). bbleh\_M2. <https://doi.org/10.5281/zenodo.1210142>
- Donatelli, C. (2018c). bbleh\_M2\_5. <https://doi.org/10.5281/zenodo.1210144>
- Donatelli, C. (2018d). bbleh\_M2\_10. <https://doi.org/10.5281/zenodo.1210146>
- Donatelli, C. (2018e). bbleh\_M2\_15. <https://doi.org/10.5281/zenodo.1210148>
- Donatelli, C. (2018f). bbleh\_M2\_20. <https://doi.org/10.5281/zenodo.1210152>
- Donatelli, C. (2018g). bbleh\_vegetation\_dieoff. <https://doi.org/10.5281/zenodo.1210192>
- Donatelli, C. (2018h). bbleh\_waves\_10. <https://doi.org/10.5281/zenodo.1228932>
- Donatelli, C. (2018i). bbleh100\_waves\_10. <https://doi.org/10.5281/zenodo.1228936>
- Donatelli, C. (2018j). bbleh\_25. <https://doi.org/10.5281/zenodo.1210166>
- Donatelli, C. (2018k). bbleh\_25\_M2. <https://doi.org/10.5281/zenodo.1210156>
- Donatelli, C. (2018l). bbleh\_50. <https://doi.org/10.5281/zenodo.1210168>

- Donatelli, C. (2018o). bbleh\_50\_M2. <https://doi.org/10.5281/zenodo.1210158>
- Donatelli, C. (2018p). bbleh\_75. <https://doi.org/10.5281/zenodo.1210170>
- Donatelli, C. (2018q). bbleh\_75\_M2. <https://doi.org/10.5281/zenodo.1210160>
- Donatelli, C. (2018r). bbleh\_100. <https://doi.org/10.5281/zenodo.1210172>
- Donatelli, C. (2018s). bbleh\_100\_M2. <https://doi.org/10.5281/zenodo.1210162>
- Donatelli, C., Ganju, N. K., Fagherazzi, S., & Leonardi, N. (2018). Seagrass impact on sediment exchange between tidal flats and salt marsh, and the sediment budget of shallow bays. *Geophysical Research Letters*, *45*, 4933–4943. <https://doi.org/10.1029/2018GL078056>
- Fagherazzi, S., Kirwan, M. L., Mudd, S. M., Guntenspergen, G. R., Temmerman, S., D'Alpaos, A., et al. (2012). Numerical models of salt marsh evolution: Ecological, geomorphic, and climatic factors. *Reviews of Geophysics*, *50*, RG1002. <https://doi.org/10.1029/2011RG000359>
- Fagherazzi, S., & Priestas, A. M. (2010). Sediments and water fluxes in a muddy coastline: Interplay between waves and tidal channel hydrodynamics. *Earth Surface Processes and Landforms*, *35*(3), 284–293. <https://doi.org/10.1002/esp.1909>
- Fagherazzi, S., Wiberg, P. L., Temmerman, S., Struyf, E., Zhao, Y., & Raymond, P. A. (2013). Fluxes of water, sediments, and biogeochemical compounds in salt marshes. *Ecological Processes*, *2*(1), 3.
- Falcini, F., Khan, N. S., Macelloni, L., Horton, B. P., Lutken, C. B., Mckee, K. L., et al. (2012). Linking the historic 2011 Mississippi River flood to coastal wetland sedimentation. *Nature Geoscience*, *5*(11), 803–807. <https://doi.org/10.1038/ngeo1615>
- Feagin, R. A., Irish, J. L., Möller, I., Williams, A. M., Colón-Rivera, R. J., & Mousavi, M. E. (2011). Engineering properties of wetland plants with application to wave attenuation. *Coastal Engineering*, *58*(3), 251–255. <https://doi.org/10.1016/j.coastaleng.2010.10.003>
- FitzGerald, D. M. (1996). Geomorphic variability and morphologic and sedimentologic controls on tidal inlets. *Journal of Coastal Research*, *81*, 47–71.
- FitzGerald, D. M., Kulp, M., Penland, P., Flocks, J., & Kindinger, J. (2004). Morphologic and stratigraphic evolution of ebb-tidal deltas along a subsiding coast: Barataria Bay, Mississippi River Delta. *Sedimentology*, *15*, 1125–1148.
- FitzGerald, D. M., Fenster, M. S., Argow, B. A., & Buynevich, I. V. (2008). Coastal impacts due to sea-level rise. *Annual Review of Earth and Planetary Sciences*, *36*(1), 601–647. <https://doi.org/10.1146/annurev.earth.35.031306.140139>
- Fortunato, A. B., & Oliveira, A. (2005). Influence of intertidal flats on tidal asymmetry. *Journal of Coastal Research*, *21*(5), 1062–1067.
- Foster, N. M., Hudson, M. D., Bray, S., & Nicholls, R. J. (2013). Intertidal mudflat and salt marsh conservation and sustainable use in the UK: a review. *Journal of Environmental Management*, *126*, 96–104.
- Friedrichs, C. T., & Aubrey, D. G. (1988). Non-linear tidal distortion in shallow well-mixed estuaries: A synthesis. *Estuarine, Coastal and Shelf Science*, *27*(5), 521–545. [https://doi.org/10.1016/0272-7714\(88\)90082-0](https://doi.org/10.1016/0272-7714(88)90082-0)
- Friedrichs, C. T., & Madsen, O. S. (1992). Non-linear diffusion of the tidal signal in frictionally dominated embayments. *Journal of Geophysical Research*, *97*, 5637–5650. <https://doi.org/10.1029/92JC00354>
- Ganju, N. K., Defne, Z., Kirwan, M. L., Fagherazzi, S., D'Alpaos, A., & Carniello, L. (2017). Spatially integrative metrics reveal hidden vulnerability of microtidal salt marshes. *Nature Communications*, *8*, 14156.
- Ganju, N. K., Nidziko, N. J., & Kirwan, M. L. (2013). Inferring tidal wetland stability from channel sediment fluxes: Observations and a conceptual model. *Journal of Geophysical Research: Earth Surface*, *118*, 2045–2058. <https://doi.org/10.1002/jgrf.20143>
- Ganju, N. K., & Sherwood, C. R. (2010). Effect of roughness formulation on the performance of a coupled wave, hydrodynamic, and sediment transport model. *Ocean Modelling*, *33*(3–4), 299–313. <https://doi.org/10.1016/j.ocemod.2010.03.003>
- Goodwin, G. C., Mudd, S. M., & Clubb, F. J. (2018). Unsupervised detection of salt marsh platforms: A topographic method. *Earth Surface Dynamics*, *6*(1), 239–255. <https://doi.org/10.5194/esurf-6-239-2018>
- Haidvogel, D. B., Arango, H. G., Budgell, W. P., Cornuelle, B. D., Curchitser, E., di Lorenzo, E., et al. (2008). Regional ocean forecasting in terrain-following coordinates: Model formulation and skill assessment. *Journal of Computational Physics*, *227*, 3595–3624.
- Haidvogel, D. B., Arango, H. G., Hedstrom, K., Beckmann, A., Malanotte-Rizzoli, P., & Shchepetkin, A. F. (2000). Model evaluation experiments in the north Atlantic basin: Simulations in nonlinear terrain-following coordinates. *Dynamics of Atmospheres and Oceans*, *17*(32), 239–281.
- Hunchak-Kariouk, K. (1999). Relation of water quality to land use in the drainage basins of four tributaries to the Toms River, New Jersey, 1994–1995. No. PB-99-149098/XAB; USGS/WRI-99-4001. Geological Survey, Water Resources Div., West Trenton, NJ (United States); New Jersey Dept. of Environmental Protection, Trenton, NJ (United States).
- Jarrett, J. T. (1976). Tidal prism-inlet area relationships. GITI Rep. 3, U.S. Army Eng. Waterw. Exp. Stn., Vicksburg, MS.
- Kalra, T. S., Aretxabaleta, A., Seshadri, P., Ganju, N. K., & Beudin, A. (2017). Sensitivity analysis of a coupled hydrodynamic-vegetation model using the effectively subsampled quadratures method. *Geoscientific Model Development*, *10*, 4511–4523.
- Kennish, M. J. (2001). State of the estuary and watershed: An overview. *Journal of Coastal Research Special Issue*, *32*, 243–273.
- Keulegan, G. H. (1967). Tidal flow in entrances, U.S. Army Corps of Engineers, Committee on Tidal Hydraulics, Tech. Bull. 14, Vicksburg.
- Knutson, P. L., Brochu, R. A., Seelig, W. N., & Inske, M. (1982). Wave damping in Spartina alterniflora marshes. *Wetlands*, *2*(1), 87–104. <https://doi.org/10.1007/BF03160548>
- Lapentina, A., & Sheng, Y. P. (2014). Three-dimensional modeling of storm surge and inundation including the effects of coastal vegetation. *Estuaries and Coasts*, *37*(4), 1028–1040. <https://doi.org/10.1007/s12237-013-9730-0>
- Lathrop, R. G. Jr., & Bognar, J. A. (2001). Habitat loss and alteration in the Barnegat Bay region. *Journal of Coastal Research*, 212–228. <https://doi.org/10.2307/25736235>
- Leonard, L. A., & Croft, A. L. (2006). The effect of standing biomass on flow velocity and turbulence in Spartina alterniflora canopies. *Estuarine, Coastal and Shelf Science*, *69*(3–4), 325–336. <https://doi.org/10.1016/j.ecss.2006.05.004>
- Leonard, L. A., & Luther, M. E. (1995). Flow hydrodynamics in tidal marsh canopies. *Limnology and Oceanography*, *40*(8), 1474–1484. <https://doi.org/10.4319/lo.1995.40.8.1474>
- Leonard, L. A., & Reed, D. J. (2002). Hydrodynamics and sediment transport through tidal marsh canopies. *Journal of Coastal Research*, *36*, 459–469.
- Leonardi, N., Carnacina, I., Donatelli, C., Ganju, N. K., Plater, A. J., Schuerch, M., & Temmerman, S. (2017). Dynamic interactions between coastal storms and salt marshes: A review. *Geomorphology*, *301*, 92–107. <https://doi.org/10.1016/j.geomorph.2017.11.001>
- Leonardi, N., Defne, Z., Ganju, N. K., & Fagherazzi, S. (2016). Salt marsh erosion rates and boundary features in a shallow bay. *Journal of Geophysical Research: Earth Surface*, *121*, 1861–1875. <https://doi.org/10.1002/2016JF003975>
- Leonardi, N., & Fagherazzi, S. (2014). How waves shape salt marshes. *Geology*, *42*(10), 887–890. <https://doi.org/10.1130/G35751.1>
- Leonardi, N., Ganju, N. K., & Fagherazzi, S. (2016). A linear relationship between wave power and erosion determines salt-marsh resilience to violent storms and hurricanes. *Proceedings of the National Academy of Sciences*, *113*(1), 64–68. <https://doi.org/10.1073/pnas.1510095112>
- List, J. H., Jaffe, B. E., Sallenger, A. H. Jr., & Hansen, M. E. (1997). Bathymetric comparisons adjacent to the Louisiana barrier islands—Processes of large-scale change. *Journal of Coastal Research*, *13*, 670–678.

- List, J. H., Jaffe, B. E., Sallenger, A. H. Jr, Williams, S. J., McBride, R. A., & Penland, S. (1994). Louisiana barrier island erosion study: Atlas of seafloor changes from 1878 to 1989. USGS/La. State University Misc. Investig. Ser. I-2150-A, USGS, Reston, VA.
- Luhar, M., & Nepf, H. M. (2011). Flow-induced reconfiguration of buoyant and flexible aquatic vegetation. *Limnol. Oceanography*, *56*(6), 2003–2017.
- Madsen, O. S. (1994). Spectral wave–current bottom boundary layer flows. In: Coastal Engineering 1994. Proceedings of the 24th International Conference on Coastal Engineering Research Council, Kobe, Japan, pp. 384–398.
- Marani, M., D'Alpaos, A., Lanzoni, S., Carniello, L., & Rinaldo, A. (2007). Biologically-controlled multiple equilibria of tidal landforms and the fate of the Venice lagoon. *Geophysical Research Letters*, *34*, L11402. <https://doi.org/10.1029/2007GL030178>
- Marani, M., D'Alpaos, A., Lanzoni, S., Carniello, L., & Rinaldo, A. (2010). The importance of being coupled: Stable states and catastrophic shifts in tidal biomorphodynamics. *Journal of Geophysical Research*, *115*, F04004. <https://doi.org/10.1029/2009JF001600>
- Marani, M., D'Alpaos, A., Lanzoni, S., & Santalucia, M. (2011). Understanding and predicting wave erosion of marsh edges. *Geophysical Research Letters*, *38*, L21401. <https://doi.org/10.1029/2011GL048995>
- Marjoribanks, T. I., Hardy, R. J., & Lane, S. N. (2014). The hydraulic description of vegetated river channels: The weaknesses of existing formulations and emerging alternatives. *WIREs Water*, *1*(6), 549–560. <https://doi.org/10.1002/wat2.1044>
- Moller, I., Spencer, T., French, J. R., Leggett, D. J., & Dixon, M. (1999). Wave transformation over tidalmarshes: A field and numerical modeling study from North Norfolk. *Estuarine, Coastal and Shelf Science*, *49*(3), 411–426. <https://doi.org/10.1006/ecss.1999.0509>
- Morin, J., Leclerc, M. M., Secretan, Y., & Boudreau, P. (2000). Integrated two-dimensional macrophytes-hydrodynamic modelling. *Journal of Hydraulic Research*, *38*(3), 163–172. <https://doi.org/10.1080/0021680009498334>
- Morris, J. T., Sundareshwar, P. V., Nietch, C. T., Kjerfve, B., & Cahoon, D. R. (2002). Responses of coastal wetlands to rising sea level. *Ecology*, *83*(10), 2869–2877. [https://doi.org/10.1890/0012-9658\(2002\)083\[2869:ROCWTR\]2.0.CO;2](https://doi.org/10.1890/0012-9658(2002)083[2869:ROCWTR]2.0.CO;2)
- Mudd, S. M., D'Alpaos, A., & Morris, J. T. (2010). How does vegetation affect sedimentation on tidal marshes? Investigating particle capture and hydrodynamic controls on biologically mediated sedimentation. *Journal of Geophysical Research*, *115*, F03029. <https://doi.org/10.1029/2009JF001600>
- Mukai, A. Y., Westerink, J. J., Luettich, R. A. Jr., & Mark, D. (2002). Eastcoast 2001: A tidal constituent database for the western North Atlantic, Gulf of Mexico and Caribbean Sea. US Army Engineer Research and Development Center, Coastal and Hydraulics Laboratory, Technical Report, ERDC/CHL TR-02-24.
- Murphy, A. H., & Epstein, E. S. (1989). Skill scores and correlation coefficients in model verification. *Monthly Weather Review*, *117*(3), 572–582. [https://doi.org/10.1175/1520-0493\(1989\)117<0572:SSACCI>2.0.CO;2](https://doi.org/10.1175/1520-0493(1989)117<0572:SSACCI>2.0.CO;2)
- Nepf, H. M. (1999). Drag, turbulence, and diffusion in flow through emergent vegetation. *Water Resources Research*, *35*, 479–489. <https://doi.org/10.1029/1998WR900069>
- O'Brien, M. P. (1931). Estuary tidal prisms related to entrance areas. *Civil Engineering*, *1*, 738–739.
- O'Brien, M. P. (1969). Equilibrium flow areas of inlets on sandy coasts. *Journal of Waterway, Port, Coastal, and Ocean Engineering*, *95*, 43–55.
- Pawlowicz, R., Beardsley, B., & Lentz, S. (2002). Classical tidal harmonic analysis including error estimates in MATLAB using T\_TIDE. *Computational Geosciences*, *28*(8), 929–937. [https://doi.org/10.1016/S0098-3004\(02\)00013-4](https://doi.org/10.1016/S0098-3004(02)00013-4)
- Picado, A., Dias, J. M., & Fortunato, A. B. (2010). Tidal changes in estuarine systems induced by local geomorphologic modifications. *Continental Shelf Research*, *30*(17), 1854–1864. <https://doi.org/10.1016/j.csr.2010.08.012>
- Ree, W. O. (1949). Hydraulic characteristics of vegetation for vegetated waterways. *Agricultural Engineering*, *30*, 184–189.
- Rodi, W. (1984). Turbulence models and their application in hydraulics—a state of the art review. Technical report, International Association of Hydraulics Research, Delft.
- Rodriguez, J. F., Saco, P. M., Sandi, S., Saintilan, N., & Riccardi, G. (2017). Potential increase in coastal wetland vulnerability to sea-level rise suggested by considering hydrodynamic attenuation effects. *Nature Communications*, *8*. <https://doi.org/10.1038/ncomms16094>
- Schwimmer, R. (2001). Rates and processes of marsh shoreline erosion in Rehoboth Bay, Delaware, U.S.A. *Journal of Coastal Research*, *17*(3), 672–683. <https://doi.org/10.1016/j.csr.2009.08.018>
- Schwimmer, R. A., & Pizzuto, J. E. (2000). A model for the evolution of marsh shorelines. *Journal of Sedimentation Research*, *70*(5), 1026–1035. <https://doi.org/10.1306/030400701026>
- Shchepetkin, A. F., & McWilliams, J. C. (2005). The Regional Ocean Modeling System: A split-explicit, free-surface, topography following coordinates ocean model. *Ocean Modelling*, *9*(4), 347–404. <https://doi.org/10.1016/j.ocemod.2004.08.002>
- Styles, R., & Glenn, S. M. (2000). Modeling stratified wave and current bottom boundary layers on the continental shelf. *Journal of Geophysical Research*, *105*, 24,119–24,139. <https://doi.org/10.1029/2000JC900115>
- Temmerman, S., Meire, P., Bouma, T. J., Herman, P. M. J., Ysebaert, T., & de Vriend, H. J. (2013). Ecosystem-based coastal defence in the face of global change. *Nature*, *504*(7478), 79–83. <https://doi.org/10.1038/nature12859>
- U.S. Department of Agriculture (2008). Plants database. Natural Resources Conservation Service. <http://plants.usda.gov/>
- Uittenbogaard, R. (2003). Modelling turbulence in vegetated aquatic flows. International workshop on Riparian Forest vegetated channels: Hydraulic, morphological and ecological aspects, Trento, Italy, 20–22 February 2003.
- Warner, J. C., Armstrong, B., He, R., & Zambon, J. B. (2010). Development of a coupled ocean-atmosphere-wave-sediment transport (COAWST) modeling system. *Ocean Modelling*, *35*(3), 230–244. <https://doi.org/10.1016/j.ocemod.2010.07.010>
- Warner, J. C., Sherwood, C. R., Signell, R. P., Harris, C., & Arango, H. G. (2008). Development of a three-dimensional, regional, coupled wave, current, and sediment-transport model. *Computers and Geosciences*, *34*(10), 1284–1306. <https://doi.org/10.1016/j.cageo.2008.02.012>
- Xiaorong, L., Plater, A., & Leonardi, N. (2018). Modelling the transport and export of sediments in macrotidal estuaries with eroding salt marsh. *Estuaries and Coasts*, 1–14. <https://doi.org/10.1007/s12237-018-0371-1>
- Yang, S. L. (1998). The role of Scirpus marsh in attenuation of hydrodynamics and retention of fine-grained sediment in the Yangtze estuary. *Estuarine, Coastal and Shelf Science*, *47*(2), 227–233. <https://doi.org/10.1006/ecss.1998.0348>